Optica Applicata, Vol. LVI, No. 1, 2026
DOI: 10.37190/oa/215064

The optical path of a multi-pass cell measured by optical frequency domain interferometry

HANCHUAN DONG[1], YUAN YIN[2], ZIHAO LI[2], JUN LI[3,4], JINBAO XIA[2,*]

[1] Technology Innovation Center for Geological Environment Monitoring, MNR, Baoding, Hebei, 071051, China

[2] Shandong University, Shanda Nanlu Road Jinan, Shandong, 250100, China

[3] CCTEG Chongqing Research Institute, Chongqing 400039, China

[4] State Key Laboratory of Coal Mine Disaster Preventing and Control, Chongqing 400037, China

The multi-pass cell (MPC) is an effective approach to extend the interaction path between laser radiation and gas molecules, thereby improving the detection sensitivity of laser-based gas sensors. However, an inaccurate determination of the MPC optical path length can introduce significant errors in direct absorption spectroscopy. In this work, we proposed a fast and precise technique —optical frequency domain interferometry (OFDI)—for measuring the MPC length, particularly suitable for configurations where the laser entrance and exit share the same window. Both the conventional absorption-based method and the proposed OFDI method were implemented and compared. Experimental results show that for a 295.4 m-long MPC, the absorption method yielded an uncertainty of approximately 1 m, while the OFDI approach reduced this to about 5 cm. Using the corrected MPC length, a carbon dioxide sensor was developed, achieving a detection sensitivity of 1.2 ppm with an integration time of 60 s. The proposed OFDI method provides a simple and highly effective solution for accurately measuring the optical path length of multi-pass cells and other optical systems.

Keywords: spectroscopy, optical frequency domain interferometry (OFDI), multipass cell laser.

1. Introduction: The manuscript

In the fields of atmospheric chemistry [1], pollution monitoring [2], and pollution prevention [3], trace gas detection is an effective method. According to the Beer–Lambert equation, increasing the interaction path is an effective way to boost the absorption signal and improve the detection sensitivity and precision for low gas concentrations. Methane, carbon dioxide, and other gases were measured using a variety of MPC types [4-7], including white cell [8] and Herriot cell [9], which have detection sensitivity of parts per million (ppm) or parts per billion (ppb) [10, 11]. The path length is a crucial parameter for the MPC, and a length error produces an inaccurate concentration. A dual beam technique in wavelength modulation spectroscopy [12] was used to get the accurate and high sensitivity measurement result, which necessitates the two beams having the same optical path. Otherwise, there will be significant amplitude residue errors due to the variations in path lengths. Estimating the number of laser beam reflections in the MPC is a straightforward and approximative approach for measuring the MPC length, but it is not very accurate and is consequently rarely employed. The length of the MPC was recovered by FIEDLER *et al.* [13] using the absorption approach, with a relative uncertainty of roughly 0.4%. REN *et al.* [14] adopted a phase difference method to measure a MPC with length of 50 m MPC achieving the uncertainty of 0.03 m. CAI and GAO [15] used the optical frequency domain reflector (OFDR) approach to get an uncertainty about 0.0085%.

The optical coherent measurement of backscattered signals from two objects, like window glasses [16] or optical fibers [17], is the foundation of the OFDR technique. This approach does not work well for the MPC with only one window, which has the same entrance and exit window, or the MPC without windows [18], but it provides two key insights: the wavelength linear sweeping and optical heterodyne are essential components for this method to be successful. Within the coherence length, two coherent signals must be received. The optical frequency domain interferometry (OFDI), a direct and easy method of measuring the MPC length, was established in this work for the measurement of the MPC optical route.

The OFDI principle is presented first in the paper. The experiment was designed to measure the coherent signal from the MPC using this methodology. By varying the injected laser current, we were able to achieve laser frequency sweeping in our experiment. By combining a short fiber in the variable arm with a long fiber of approximately 248.2 meters in the fixed arm and an optical path of 345.6 meters in the air, equivalent coherence lengths in the two arms were accomplished. When the variable arm's length is altered, the beat frequency of the interference from the two arms is used to compute the MPC length, which was determined to be 296.4 meters.

2. Principle and experiment

2.1. Principle

The OFDR methodology served as the basis for the modification of the OFDI method. The optical coherence of the fiber's backscattering signal is the basis for the OFDR principle. A fiber coupler separates the laser beam into a fixed arm and a measuring arm in an OFDI system. The interference beating of the two beams happens with the tunable laser frequency sweeping, and the beat frequency of the signal's FFT is used to determine the time delay or length difference. The principle is illustrated in Fig. 1.

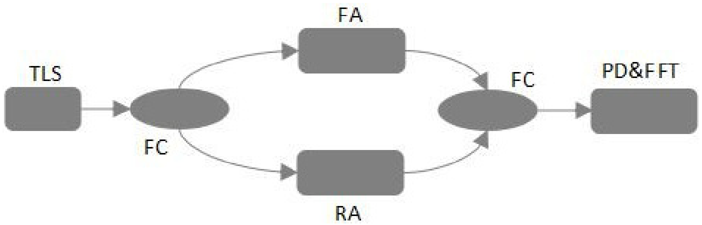

Fig. 1. The principle of OFDI. TLS: tunable laser source, FC: fiber couple, FA: fixed arm, RA: reference arm, and PD: photodiode.

The electromagnetic wave in the fixed arm (fiber) and reference arm (MPC) is expressed as

$$E_0(t) = E_f \exp(i\varphi(t)) \tag{1}$$

$$E_1(t) = E_m(t)\exp(i\varphi(t-t_0)) \tag{2}$$

where E_f and $E_m(t)$ are the amplitude of the signals, $\varphi(t)$ is the signal phase of the function of time and t_0 is the time delay in reference channel. When the laser source was scanned with frequency speed γ, under the assumption of the phase of signal being linear increasing, the beat signal at the detector is expressed by the following equation

$$I_0(t) = I_c \cos\left(\gamma t_0 t + \frac{1}{2}\gamma t_0^2 - \omega_0 t_0\right) \tag{3}$$

where ω_0 is the initial frequency, $I_c(t)$ is the signal intensity on the detector, $I_0(t)$ is the beat signal. The center frequency γt_0 can be obtained from the Fourier transformation of the beat signal, then the time delay t_0 can be calculated. The length of MPC can be calculated by $t_0 C$ ($C = 3 \times 10^8$ m/s).

In the experiment we only employed a short fiber (fixed arm) and a longer fiber (reference arm, which was 20 meters longer than the short fiber) to test the idea. Figure 2 displayed the beat signal in both the time and frequency domains. As seen in the subfigure, the cos signal with an amplitude ranging from 0.05 to 0.10 V was chosen from 0.4 to 0.5 s. With a center frequency of 137 Hz and a signal to noise ratio of about 20 dB, the beat frequency was fitted to have a Gaussian shape. It demonstrates the viability of the idea.

2.2. Experiment setup

Figure 3 displays the system diagram. A distributed feedback (DFB) diode laser, whose wavelength can be tuned from 1604.8 to 1605.8 nm at 25°C, serves as the system's tunable source. A commercial laser controller (ILX Lightwave LDC3714C) controls the laser's temperature and current. The DAQ Card (NI-USB-6211,National Instrument)

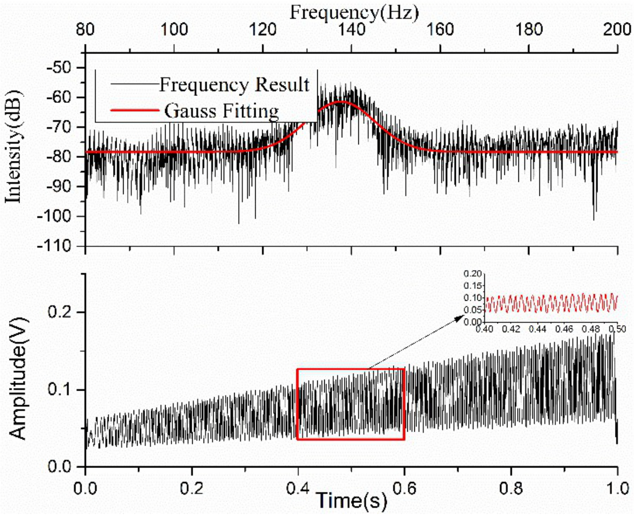

Fig. 2. The verification of the principle by two fibers.

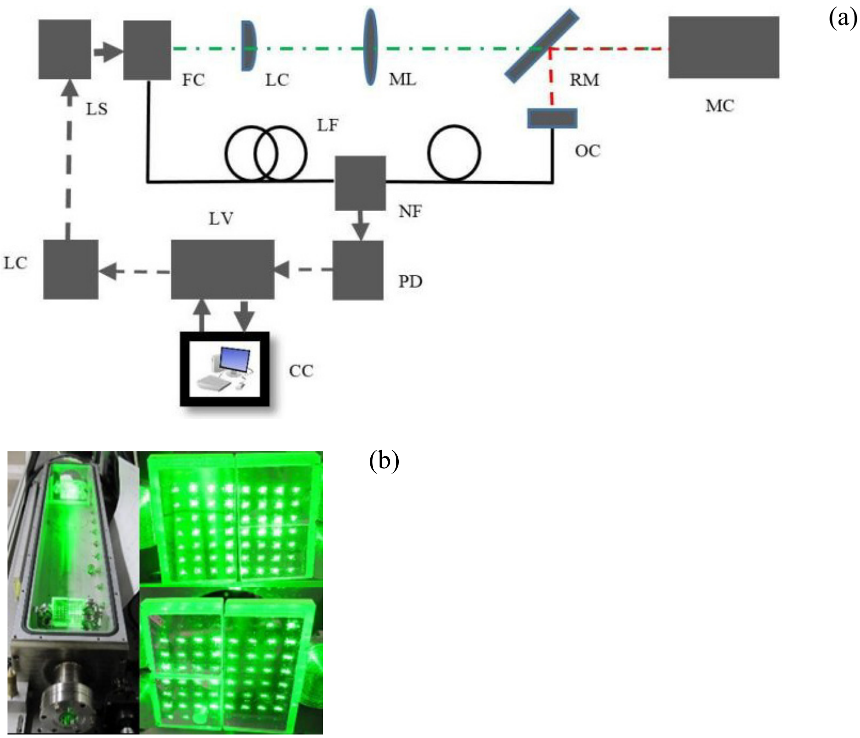

Fig. 3. A schematic diagram of our OFDI setup for measuring length. (a) LV: NI card, LC: laser controller, LS: laser source, FC: 99/1 fiber coupler, LC: laser collimator, ML: mode matching lens, RM: reflective mirror, OC: optical coupler, LF: long fiber, NF: nonlinear fiber, PD: photodiode, CC: control computer. (b) The designed multipass cell.

generates a ramp signal that is managed by LabVIEW software and transmitted to the laser controller via a voltage follower that solves current matching. The voltage amplitude increased from 2 to 10 V, which translates into a laser current that corresponds from 20 to 100 mA, while the sweeping frequency is 2 Hz. The laser beam is divided into a reference arm, consisting of a 248.2 m long fiber, and a signal arm. A fiber-coupled collimator (Thorlabs, $f = 4.8$ mm) is used to collimate the signal beam, which then enters the MPC. After being mode-matched by a lens with a 10 mm focal length, the beam undergoes approximately 500 reflections within the cell. The output from the MPC is coupled into a short optical fiber. A nonlinear polarization-maintaining fiber then combines the signals from the two arms and provides the necessary polarization correction. This nonlinear fiber effectively mitigates polarization state inconsistencies arising from light transmission and reflection. It ensures that the two beams meet the polarization conditions necessary for effective interference and performs polarization correction simultaneously, thereby achieving stable interference, reducing experimental errors, and improving sensor sensitivity. An InGaAs photodiode (PD) (Thorlabs, FGA01-FC-PD) detects the signal, and the same DAQ Card records it. LabVIEW software processes the input, and FFT converts it into the frequency domain.

2.3. Absorption spectroscopy method and experiment

To verify our measurement result with OFDI, the absorption spectroscopy method was used to get the length of the MPC. The absorption spectroscopy method is based on the Beer–Lambert law, which is described by the expressions

$$I_0 = I_i \exp(-s g(v, P, T) L) \quad (4)$$

$$L = -\frac{1}{s g(v, P, T)} \ln \frac{I_0}{I_i} \quad (5)$$

Here I_0 and I_i are the incident and the transmitted laser powers, L is the length of the MPC, s is the spectral line intensity, $g(v, P, T)$ is the normalized line shape function, which can be Gaussian or Lorentzian profile function depending on the temperature T and pressure P.

Some components had to be changed for the absorption experiment. The nonlinear fiber and the long reference fiber were removed from the setup. A low-pass filter was applied to the photodiode's signal in order to eliminate noise. The laser controller in this experiment was likewise controlled by commands from the LabVIEW program. The mode-matching lens and laser collimator were used to transmit the laser beam into the MPC. The output signal from MPC was detected by a photodiode, then filtered by a low pass filter and sampled by a digital acquisition card.

In the experiment, we firstly flushed the nitrogen gas into the MPC for about twenty minutes until no air in the chamber. After that, we injected multi-concentrations calibrated gas of carbon dioxide (CO_2), and methane (CH_4) with concentrations of 510 ppmV,

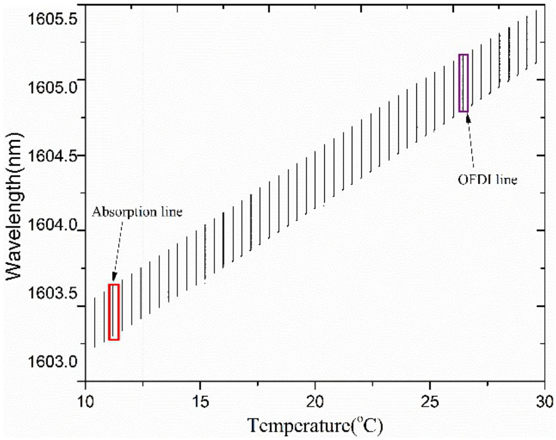

Fig. 4. The wavelength *versus* the temperature.

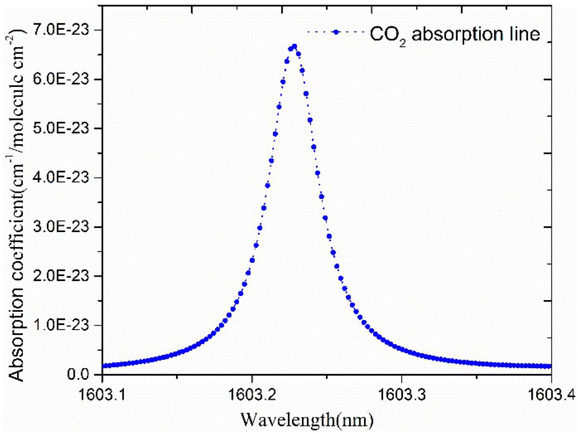

Fig. 5. The chosen absorption lines from the HITRAN database.

2.010 ppmV and got the absorption concentration as the experiment procedure mentioned in the paper.

A wavemeter (Burleigh Wav-1500) was used to firstly calibrate the relationship between temperature and the DFB laser scanning wavelength in the absorption method experiment, as seen in Fig. 4. In the Fig. 5, the carbon dioxide absorption lines with a central wavelength of 1603.24 nm were selected from the HITRAN 2008 database [19]. The absorption wavelength seen in the Fig. 4 is covered by the laser at 11.4 degrees.

3. Result and discussion

FFT is used to evaluate the data in the frequency domain of the OFDI experiment, and the computed result is displayed in Fig. 6. According to the figure, the beat frequency spanned the frequency range of 3 to 5 MHz, with a central wavelength of 3.76 MHz

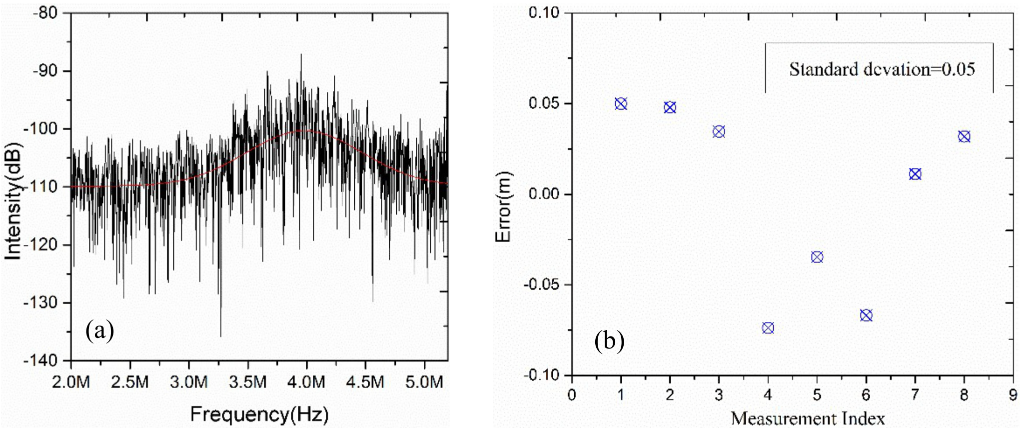

Fig. 6. The beat frequency signal and the amplifier frequency characteristic.

and a profile fitted as a Gaussian function. Due to the MPC noise and the reduced optical signal on the detector, the SNR dropped to 10 dB. The length difference between the MPC and long fiber was determined to be 14.29 meters using Eq. (3). By multiplying the fiber's refractive index of 1.4475 by its length of 248.2 meters, the effective optical length of a long fiber was 359.27 meters. The effective length of the MPC was 293.61 meters after deducting the open path length and the short fiber in the fixed arm of our testing setup. We conducted this experiment eight times in order to compute the result errors, and the mistakes are displayed in Fig. 7. The length's uncertainty is 5 cm, as indicated by the standard deviation value of 0.05.

The room temperature and pressure for the absorption method are measured to be 290 K and 760 Torr, respectively. For the measurement of the carbon dioxide absorption line shown in Fig. 7, the lines in Fig. 5 were chosen. As seen in Fig. 7, the outcome is fitted using the Voigt profile [19]. The horizontal axis represents time, and the vertical

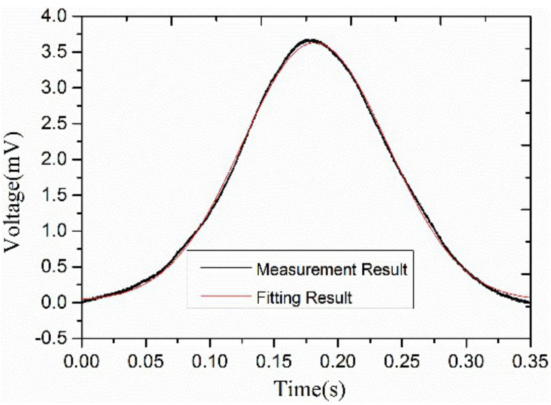

Fig. 7. Absorption lines measured by absorption method.

axis represents the voltage of the absorption signal. Results from three experiments were conducted. Since their respective readings are 295.5, 294.5, and 296.4 meters, the uncertainty is roughly one meter. Even with the use of a balanced detector in the absorption method, certain noises were still challenging to eliminate. The OFDI approach outperforms the phase detection method in terms of accuracy, improving the MPC from meter to centimeter when compared to the absorption method. In actuality, the mistakes in this finding are more than those in the OFDR approach. The following succinctly describes the reason of errors.

The first is the imprecision of the fibers' precise refractive index values. Our computation makes advantage of the refractive index's nominal value. About 2 cm of mistakes can result from a 0.001 relative refractive index error. Second, the MPC's interior is not the entire optical path. With the fixed arm's small open route and fiber, it is challenging to obtain the length with an accuracy of less than a centimeter. Third, the main issue is that, in contrast to the special lasers used in the OFDR method for measuring

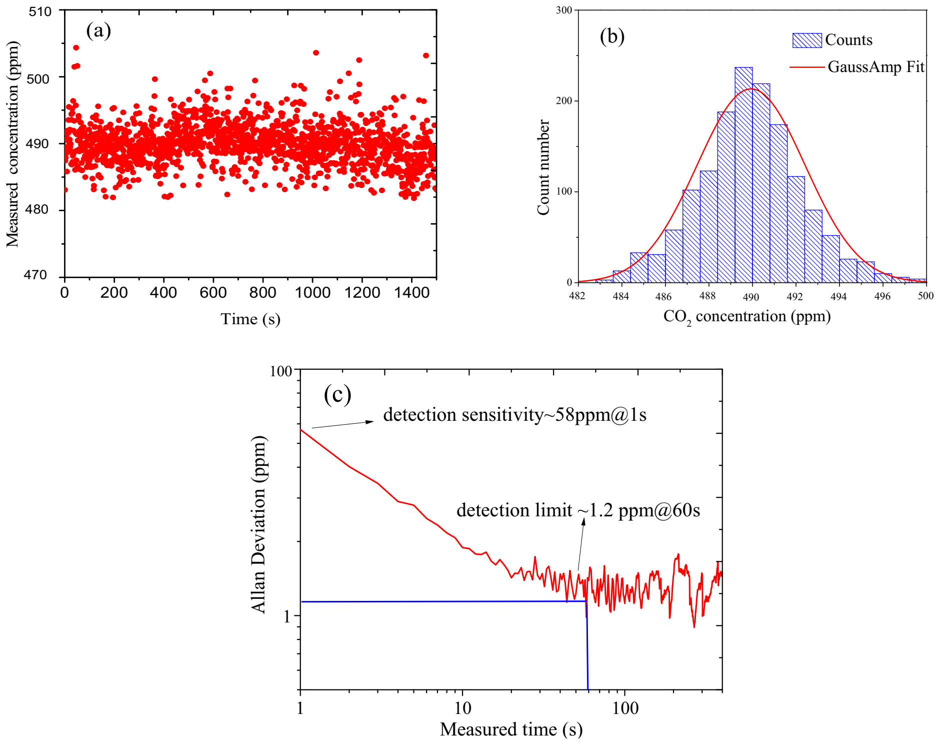

Fig. 8. Results of the sensor tests: (a) The results for a 25 minutes continuous data acquisition with 490 ppm carbon dioxide concentration mixture. (b) The histogram of the measured data points. (c) The Allan deviation of the measured data, showing the detection limits of 58 and 1.2 ppm with averaging times of 1 and 60 s, respectively.

thousands of distances, the DFB laser's spectrum in our experiment contains additional peaks that obstruct the coherent result and its linewidth is insufficiently narrow.

To further evaluate the measurement precision of the sensor, a long-term continuous experiment was carried out with the 200 ppm calibration carbon dioxide gas mixture at a total pressure of 760 Torr and room temperature. During continuous measurement for twenty-five minutes with 1s interval 1500 data points were obtained (Fig. 8(a)). The histogram plot of the measured data shows data distribution in Fig. 8(b). The distribution was fitted by a Gaussian profile and the HWHM value was determined to be 6.2 ppm. Thus, the relative error of the acetone concentration measurement is 0.3%. The uncertainty in the measured concentration value can be mainly attributed to electronic noise.

To investigate the detection limit and stability of the sensor, the Allan deviation analysis was performed, as depicted in Fig. 8(c). The results indicate that the sensitivity is about 58 ppm with 1 s averaging time and reaches the optimal sensitivity of the sensor of 1.2 ppm when the integration time is increased to 60 s. For integration times longer than the optimal one, the Allan deviation increases due to drift and the noise of the laser and electronic components. The noise can be further suppressed to improve the sensor sensitivity by using a balanced detection.

4. Conclusion

Different techniques can be used to measure the length of the cells of different types with different precision. The absorption method was also tested for our unique MPC, yielding an approximate length of 295 meters with a 1-meter margin of error. A DFB laser with a linewidth of 5 MHz and a long fiber of 248 meters was used to implement the OFDI technique idea in our work in order to increase the length accuracy. The length precision is increased by 20 scales with this method, from one meter to five centimeters. This technique can also be used to measure the length of other optical cells or distance. To further increase the accuracy, we will address some of the aforementioned error causes in our next stage. The experiment for carbon dioxide was also carried out with the sensitivity of 1.2 ppm with integration time of 60 seconds.

Acknowledgments
This work was supported by the Open Funding of Technology Innovation Center for Geological Environment Monitoring (2020KFK1212002), the Fundamental Research Funds for the Central Universities (grant numbers 11621418 and 21617349), and the open funding of State Key Laboratory of Coal Mine Disaster Prevention and Control (grant no. 2024SKLKF07).

References

[1] Lashof D.A., Ahuja D.R., *Relative contributions of greenhouse gas emissions to global warming*, Nature, **344**(6266), 1990: 529–531. https://doi.org/10.1038/344529a0

[2] ALLEN D.T., SMITH D., TORRES V.M., SALDANA F.C., *Carbon dioxide, methane and black carbon emissions from upstream oil and gas flaring in the United States*, Current Opinion in Chemical Engineering, **13**, 2016: 119–223. https://doi.org/10.1016/j.coche.2016.08.014

[3] LIU Y., MA Y., *Advances in multipass cell for absorption spectroscopy-based trace gas sensing technology [Invited]*, Chinese Optics Letters, **21**(3), 2023: 033001.

[4] FATHY A., SABRY Y.M., HUNTER I.W., KHALIL D., BOUROUINA T., *Direct absorption and photoacoustic spectroscopy for gas sensing and analysis: A critical review*, Laser & Photonics Reviews, **16**(8), 2022: 2100556. https://doi.org/10.1002/lpor.202100556

[5] KONG R., SUN T., LIU P., ZHOU X., *Optical design and analysis of a two-spherical-mirror-based multipass cell*, Applied Optics, **59**(6), 2020: 1545–1552. https://doi.org/10.1364/AO.381632

[6] CHENG G., CAO Y.-N., TIAN X., CHEN J.-J., WANG J.-J., *Design and analysis of novel folded optical multi-pass cell*, Frontiers in Physics, **10**, 2022: 907715. https://doi.org/10.3389/fphy.2022.907715

[7] FRANCO B., MAHIEU E., EMMONS L.K., TZOMPA-SOSA Z.A., FISCHER E.V., SUDO K., BOVY B., CONWAY S., GRIFFIN D., HANNIGAN J.W., *Evaluating ethane and methane emissions associated with the development of oil and natural gas extraction in North America*, Environmental Research Letters, **11**(4), 2016: 044010. https://doi.org/10.1088/1748-9326/11/4/044010

[8] WHITE J.U., *Long optical paths of large aperture*, Journal of the Optical Society of America, **32**(5), 1942: 285–288. https://doi.org/10.1364/JOSA.32.000285

[9] HERRIOTT D.R., SCHULTE H.J., *Folded optical delay lines*, Applied Optics, **4**(8), 1965: 883–889. https://doi.org/10.1364/AO.4.000883

[10] PHILIPPE L.C., HANSON R.K., *Laser diode wavelength-modulation spectroscopy for simultaneous measurement of temperature, pressure, and velocity in shock-heated oxygen flows*, Applied Optics, **32**(30), 1993: 6090–6103. https://doi.org/10.1364/AO.32.006090

[11] BEHERA A., WANG A.B., *Calibration-free wavelength modulation spectroscopy: symmetry approach and residual amplitude modulation*, Applied Optics, **55**(16), 2016: 4446–4455. https://doi.org/10.1364/AO.55.004446

[12] CROSSON E.R., *A cavity ring-down analyzer for measuring atmospheric levels of methane, carbon dioxide, and water vapor*, Applied Physics B, **92**, 2008: 403–408. https://doi.org/10.1007/s00340-008-3135-y

[13] FIEDLER S.E., HESE A., RUTH A.A., *Incoherent broad-band cavity-enhanced absorption spectroscopy*, Chemical Physics Letters, **371**(3-4), 2003: 284–294. https://doi.org/10.1016/S0009-2614(03)00263-X

[14] REN W., JIANG W.Z., TITTEL F.K., *Single-QCL-based absorption sensor for simultaneous trace-gas detection of CH_4 and N_2O*, Applied Physics B, **117**, 2014: 245–251. https://doi.org/10.1007/s00340-014-5828-8

[15] CAI T.D., GAO G.Z., WANG M.R., *Simultaneous detection of atmospheric CH_4 and CO using a single tunable multi-mode diode laser at 2.33 μm*, Optics Express, **24**(2), 2016: 859–873. https://doi.org/10.1364/OE.24.000859

[16] YU Y., SANCHEZ N.P., GRIFFIN R.J., TITTEL F.K., *CW EC-QCL-based sensor for simultaneous detection of H_2O, HDO, N_2O and CH_4 using multi-pass absorption spectroscopy*, Optics Express, **24**(10), 2016: 10391–10401. https://doi.org/10.1364/OE.24.010391

[17] DONG L., TITTEL F.K., LI C., SANCHEZ N.P., WU H., ZHENG C., YU Y., SAMPAOLO A., GRIFFIN R.J., *Compact TDLAS based sensor design using interband cascade lasers for mid-IR trace gas sensing*, Optics Express, **24**(6), 2016: A528–A535. https://doi.org/10.1364/OE.24.00A528

[18] KREUZER L.B., *Ultralow gas concentration infrared absorption spectroscopy*, Journal of Applied Physics, **42**(7), 1971: 2934–2943. https://doi.org/10.1063/1.1660651

[19] ROTHMAN L.S., GORDON I.E., BARBE A., BENNER D.C., BERNATH P.F., BIRK M., BOUDON V., BROWN L.R., CAMPARGUE A., CHAMPION J.-P., CHANCE K., COUDERT L.H., DANA V., DEVI V.M., FALLY S., FLAUD J.-M., GAMACHE R.R., GOLDMAN A., JACQUEMART D., KLEINER I., LACOME N., LAFFERTY W.J., MANDIN J.-Y., MASSIE S.T., MIKHAILENKO S.N., MILLER C.E., MOAZZEN-AHMADI N., NAUMENKO O.V.,

NIKITIN A.V., ORPHAL J., PEREVALOV V.I., PERRIN A., PREDOI-CROSS A., RINSLAND C.P., ROTGER M., ŠIMEČKOVÁ M., SMITH M.A.H., SUNG K., TASHKUN S.A., TENNYSON J., TOTH R.A., VANDAELE A.C., VANDER AUWERA J., *The HITRAN 2008 molecular spectroscopic database*, Journal of Quantitative Spectroscopy and Radiative Transfer, **110**(9-10), 2009: 533–572. https://doi.org/10.1016/j.jqsrt.2009.02.013

Received September 16, 2025
in revised form November 17, 2025